Preprints.org

Article

Not peer-reviewed version

Quantum Information Copy Time (QICT): Global Predictions and Falsification Atlas

Sacha Mohamed *

Posted Date: 13 January 2026

doi: 10.20944/preprints202601.0917.v1

Keywords: Quantum Information Copy Time (QICT); falsification Atlas; Higgs-portal singlet-scalar dark matter; m_χ = 58.4 ± 6.0 GeV; dark-energy equation-of-state w_Q; copy-horizon L_{copy}; discrete Regge action; audit depth $D_{audit} \geq 7$; golden relation calibration; arrival-time lags; Helstrom advantage; Functional Renormalization Group (FRG) et effective diffusion D

Preprints.org (www.preprints.org) | NOT PEER-REVIEWED | Posted: 13 January 2026 doi:10.20944/preprints202601.0917.v1

Article

Quantum Information Copy Time (QICT): Global Predictions and Falsification Atlas

Sacha Mohamed

Independent Researcher, Casablanca, Morocco; www.sachamed@gmail.com

Abstract

We compile the falsifiable predictions stated across the Quantum Information Copy Time (QICT) preprint series into a single referee-usable atlas. Each entry is recorded as an observable statement with (i) an explicit numerical value or band when available, (ii) a minimal hypothesis set, and (iii) a concrete falsification route. The atlas is conservative: it standardizes notation and uncertainty conventions (e.g., explicit 1σ bands) without introducing additional modeling beyond what is stated in the sources.

Keywords: Quantum Information Copy Time (QICT); falsification Atlas; Higgs-portal singlet-scalar dark matter; $m_\chi = 58.4 \pm 6.0$ GeV; dark-energy equation-of-state w_Q; copy-horizon L_{copy}; discrete Regge action; audit depth $D_{audit} \geq 7$; golden relation calibration; arrival-time lags; Helstrom advantage; Functional Renormalization Group (FRG) et effective diffusion D

1. How to Read This Atlas

This manuscript is a prediction ledger. Each entry is constrained to include: (i) a named **observable**, (ii) a **prediction** as a number/band or as a sharp structural statement, (iii) a **minimal hypothesis set**, and (iv) a **falsification route** (what would rule it out under the stated hypotheses).

2. Summary Tables (Margin-Safe)

2.1. Quantitative Predictions (Explicit Numerical Bands)

Table 1. Quantitative predictions with explicit numerical bands.

ID	Observable	Prediction
DM-1	Higgs-portal singlet-scalar dark-matter mass m_χ (or m_S)	$m_\chi = 58.4 \pm 6.0$ GeV (1σ).
DM-2	Spin-independent DM–nucleon cross section $\sigma_{\rm SI}$ for Higgs-portal singlet	$\sigma_{\rm SI} \sim 5 \times 10^{-47} - 2 \times 10^{-46}$ cm^2 for representative viable points near Higgs resonance; correlated with m_S band.
DM-3	$\mathrm{BR}(h \to SS)$ for $m_S < m_h/2$	$\mathrm{BR}(h \to SS) \lesssim 10^{-3}$ in the QICT–FRG band (for allowed scan points).
DE-2	$c_Q(z) := H(z)\, L_{\rm copy}(z) \sqrt{\Omega_Q(z)}$ satisfies $c_Q(z) \leq 1$ (severe inequality)	Universal bound $c_Q(z) \leq 1$ for any admissible $\tau_{\rm copy}$ consistent with locality (no superluminal copy-horizon propagation).
DE-3	Background expansion $H(z)$ given a constant effective diffusion D	If $\tau_{\rm copy}(L) \approx L^2/(4D)$ and $c_Q \to 1$, then $L_{\rm copy} = 2\sqrt{D/H}$ and Friedmann closure yields a cubic equation for $H(z)$.

 doi:10.20944/preprints202601.0917.v1

Table 1. *Cont.*

ID	Observable	Prediction
DE-4	Dark-energy equation-of-state $w_Q(a)$	$w_Q(a) = -1 - \frac{1}{3}\,\mathrm{d}\ln\Omega_Q/\mathrm{d}\ln a$ (and hence fixed once $L_{\mathrm{copy}}(a)$ is specified).
GR-1	Discrete gravitational action and field equations	$S_{\mathrm{Regge}}[\ell] = \frac{1}{8\pi G}\sum_h A_h(\ell)\,\delta_h(\ell) - \frac{\Lambda}{8\pi G}\sum_\sigma V_\sigma(\ell)$; varying w.r.t. ℓ_e gives discrete Einstein equations.
LAB-2	Scaling of τ_{copy} with distance L	In diffusive closure, $\tau_{\mathrm{copy}}(L) \propto L^2/(\mathrm{const}\times D_{\mathrm{eff}})$ with D_{eff} extracted from a second-moment spectral susceptibility.
MASS-1	Threshold for matter-sector audit depth D_{audit}	A minimum audit depth $D_{\mathrm{audit}} \geq 7$ in 3+1D for stable matter excitations (as defined in the QICT audit framework).
ASTRO-1	Relative arrival-time lags between photon energies from compact-object flares / high-z transients	If the transient copy-horizon sector is nonzero, $\delta t(E,z)$ exhibits an energy dependence whose redshift integral is controlled by $H(z)$ and the copy-horizon epoch; applicable to EHT-band flare timing, AGN variability, and GRBs.
MASS-3	Collider exclusion lower bounds highlighting a characteristic heavy mass scale	Highlighted scales cluster into a small discrete set and shift with audit depth $D_{\min}$ approximately as $m_* \propto (D_{\min}\tau_{\min})^{-1/2}$ on the plateau $m_*c^2 = \hbar\theta/(2D_{\min}\tau_{\min})$.
CONST-1	Dimensionless combination $\chi_Y^{(2)}T_*^2$ used in the Golden Relation calibration layer	$\chi_Y^{(2)}T_*^2 = 0.145 \pm 0.010$ (benchmark prior).
CONST-2	κ_{eff} entering the Golden Relation calibration layer	$\kappa_{\mathrm{eff}} = 0.136 \pm 0.019$ (benchmark prior).
CONST-3	C_Λ constant used in Golden Relation mapping to m_S	$C_\Lambda = 1.6 \pm 0.2\ \mathrm{GeV}^{-1}$ (benchmark prior).
ASTRO-2	Energy-dependent arrival-time residuals after source-intrinsic lag marginalization	If the transient sector is present, residual lags must follow a redshift-integral kernel fixed by the same $H(z)$ and $L_{\mathrm{copy}}(z)$ that fit background expansion; purely source-local models cannot mimic the predicted z-dependence across populations.

2.2. Structural Predictions (Model-Class Constraints and Inequalities)

Table 2. Structural predictions (selected).

ID	Observable	Prediction
DE-1	$L_{\mathrm{copy}}(t)$ defined by $\tau_{\mathrm{copy}}(L_{\mathrm{copy}},t) = H^{-1}(t)$	Existence and uniqueness of L_{copy} under mild monotonicity; sets an IR scale without an event-horizon postulate.
GR-2	Quantum-gravity path integral over information configurations	$Z = \sum_C \int \prod_e \mathrm{d}I_e \prod_e \mathrm{d}n_e\ \exp\big(-S_I[I,n]\big)$ defines a nonperturbative quantum theory; classical GR appears only as a macroscopic phase.
GR-3	Universality-class statement for long-distance correlators	If RG flow has an attractive IR fixed point in the $(\tilde{G},\tilde{\Lambda})$ plane, diffeomorphism-invariant correlators converge to continuum GR in the scaling limit.

 doi:10.20944/preprints202601.0917.v1

Table 2. *Cont.*

ID	Observable	Prediction
LAB-1	$\tau_{\text{copy}}(A \to B; \eta)$ in many-body dynamics	Earliest t such that the trace distance between reduced states on B exceeds η; equivalently, the optimal Helstrom advantage is $\geq \eta$.
DCA-1	Permutation-unitary lift of reversible local update rules	In the limit of minimal update time, reversible deterministic rules correspond to permutation unitaries acting on Hilbert-space lifts.
DE-6	Consistency between expansion, growth/lensing, and transient timing observables under one inferred copy horizon $L_{\text{copy}}(z)$	A single inferred $L_{\text{copy}}(z)$ (equivalently $c_Q(z)$) must fit (i) $H(z)$ expansion data, (ii) growth/lensing reconstructions, and (iii) a transient timing observable; failure of joint consistency falsifies the copy-horizon mapping.
GR-4	Recovery of Regge-type equations and continuum GR correlators from a discrete information-field partition function	A single microscopic model yields (i) discrete field equations by exact variation and (ii) continuum Einstein dynamics as an IR scaling phase without semiclassical input; deviations must be computable and suppressed by the coarse-graining scale.

2.3. Semi-Quantitative Predictions (Scaling/Sign Constraints)

Table 3. Semi-quantitative predictions (selected).

ID	Observable	Prediction

3. Figures (Embedded in the PDF)

All figures are included directly in this PDF. They can be regenerated locally by running:

```
python3 run_everything.py
```

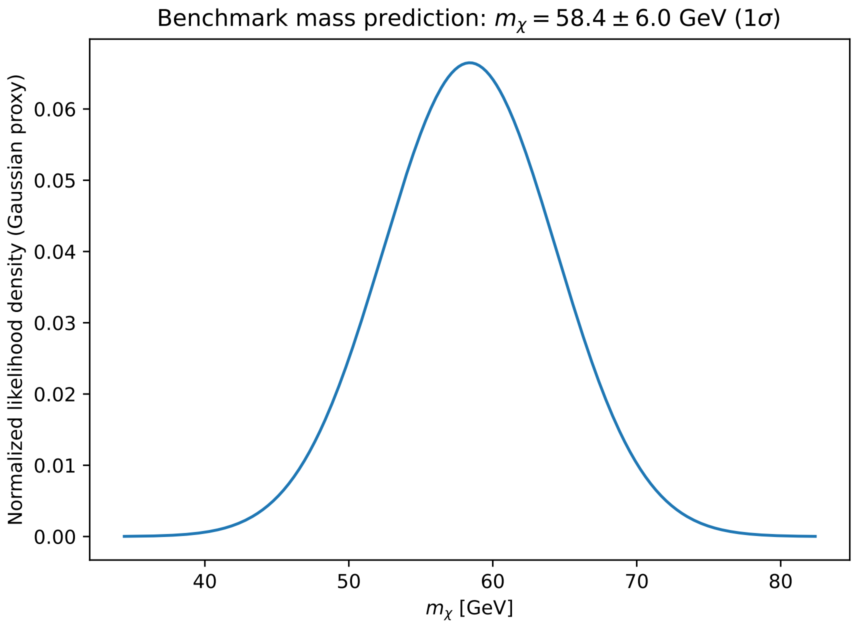

Figure 1. Visualization of the benchmark mass prediction $m_\chi = 58.4 \pm 6.0$ GeV (Gaussian proxy).

 doi:10.20944/preprints202601.0917.v1

Appendix A. Full Predictions Ledger (Assumptions and Falsification)

Table A1. Full ledger (observable, prediction, falsification) with assumptions and sources.

ID	Observable	Prediction	Falsification route
DM-1	Higgs-portal singlet-scalar dark-matter mass m_χ (or m_S)	$m_\chi = 58.4 \pm 6.0$ GeV (1σ).	If combined DD+collider+invisible-Higgs constraints exclude all viable Higgs-portal points in a ± 1 GeV band around 58.4 GeV while the pipeline premises hold, the benchmark fails.
	Assumptions: Operational τ_{copy} certificate; IR window mapping $\Lambda_{IR} \approx 2\pi/\tau_{copy}$; thermal 'copy-limited' saturation near EW crossover; minimal FRG truncation for gravity+SM+ν+singlet scalar. Uncertainty fixed to ± 6.0 GeV. *Sources:* preprints202512.2391.v3; preprints202511.2241.v3; QICT DM likelihood write-up.		
DM-2	Spin-independent DM–nucleon cross section σ_{SI}	$\sigma_{SI} \sim 5 \times 10^{-47}$–$2 \times 10^{-46}$ cm^2 for points near Higgs resonance	Future multi-ton direct detection + Higgs invisible bounds exclude $m_S \in [56, 60]$ GeV with $\sigma_{SI} \gtrsim 3 \times 10^{-47}$ cm^2.
	Assumptions: Minimal Higgs-portal with quartic coupling λ_{HS}; relic density fixed to Planck; standard Higgs-mediated SI scattering. *Sources:* preprints202511.2241.v3 (Eq. 74; Table IV; Sec. D, Eq. 85; Figs. 4–5)		
DM-3	BR(h→SS) for $m_S < m_h/2$	BR(h→SS) $\lesssim 10^{-3}$ in the QICT–FRG band	Future lepton-collider per-mille Higgs width measurement or invisible-decay searches exclude BR at $O(10^{-3})$.
	Assumptions: Same Higgs-portal parameter points as DM-2; Higgs total width constraints. *Sources:* preprints202511.2241.v3 (Eq. 84; Sec. D)		
DE-1	$L_{copy}(t)$ defined by $\tau_{copy}(L_{copy}, t) = H^{-1}(t)$	Existence/uniqueness of L_{copy} under mild monotonicity	Find a cosmological epoch where no monotone solution exists or τ_{copy} violates locality bounds.
	Assumptions: $\tau_{copy}(L, t)$ monotone increasing in L; locality + CPTP contraction; cosmological background with $H(t)$. *Sources:* preprints202601.0639.v1 (definition; Sec. 2–3)		
DE-2	$c_Q(z) := H(z)L_{copy}(z)\sqrt{\Omega_Q(z)} \leq 1$	Universal bound $c_Q(z) \leq 1$ for any admissible τ_{copy}	Observational inference demands $c_Q(z) > 1$ robustly across datasets.
	Assumptions: Locality-preserving microdynamics; identification of Ω_Q via L_{copy}. *Sources:* preprints202601.0639.v1 (Sec. 4; 'severe inequality' statement)		
DE-3	Background expansion $H(z)$ with constant diffusion D	If $\tau_{copy}(L) \approx L^2/(4D)$ and $c_Q \to 1$ then Friedmann closure yields cubic equation for $H(z)$	If $H(z)$ data cannot be fit for any D consistent with micro estimates from τ_{copy} in lab systems.
	Assumptions: Hydrodynamic/diffusive regime; single dominant diffusion constant D; saturation $c_Q \approx 1$. *Sources:* preprints202601.0639.v1 (Sec. 5–6; diffusive branch)		
DE-4	Dark-energy equation-of-state $w_Q(a)$	$w_Q(a) = -1 - (1/3)d\ln\Omega_Q/d\ln a$	Empirical reconstruction of $w(a)$ and $\Omega_Q(a)$ violates the relation.
	Assumptions: Definition of Ω_Q from L_{copy}; standard continuity equation. *Sources:* preprints202601.0639.v1 (Sec. 4; w_Q formula)		
DE-5	Energy-dependent time delay $\delta t(E, z)$	Transient sector induces energy-dependent dispersion; correlates with $L_{copy}(t)$	No correlated dispersion at predicted redshift windows.
	Assumptions: Presence of transient sector in $\tau_{copy}(L, t)$ beyond pure diffusion. *Sources:* preprints202601.0639.v1 (Sec. 7)		

Preprints.org (www.preprints.org) | NOT PEER-REVIEWED | Posted: 13 January 2026 doi:10.20944/preprints202601.0917.v1

ID	Observable	Prediction	Falsification route
GR-1	Discrete gravitational action	$S_{Regge}[\ell] = \frac{1}{8\pi G}\sum A_h\delta_h - \frac{\Lambda}{8\pi G}\sum V_\sigma$	Show microscopic action does not reduce to Regge form in any regime.
	Assumptions: Discrete information-field model on complexes; expansion around small curvature.		
	Sources: QICT_Supplement_Microscopic_GR.pdf (Eq. 5–6)		
GR-2	Quantum gravity path integral	$Z = \sum \int d\mathit{Idn} \exp(-S_I)$ defines nonperturbative theory	Demonstrate inconsistency (non-normalizable measure) or absence of GR-like scaling.
	Assumptions: Sum over complexes implements background independence.		
	Sources: QICT_Supplement_Microscopic_GR.pdf (Eq. 7; Sec. 4–5)		
GR-3	Universality-class statement	RG flow attractive IR fixed point in $(\tilde{G}, \tilde{\Lambda})$ plane	Numerical lattice studies show no such IR fixed point or different universality class.
	Assumptions: Existence of fixed point; suitable coarse-graining map B.		
	Sources: QICT_Supplement_Microscopic_GR.pdf (Sec. 5)		
LAB-1	$\tau_{copy}(A \to B; \eta)$ in many-body dynamics	Trace distance between reduced states on B exceeds η	Operational definition is ill-posed in physically relevant models (e.g., superselection).
	Assumptions: Receiver-restricted measurement class; fixed η.		
	Sources: preprints202601.0364.v1 (definition)		
LAB-2	Scaling of τ_{copy} with distance L	$\tau_{copy}(L) \propto L^2/(const \times D_{eff})$	Quantum-simulator measurement shows τ_{copy} scaling inconsistent with D_{eff} from transport.
	Assumptions: Diffusion dominates transport; SDC satisfied.		
	Sources: preprints202601.0364.v1 (hydrodynamic closure)		
DCA-1	Permutation-unitary lift	Reversible deterministic rules correspond to permutation unitaries	Show micro update rules require non-permutation unitaries at $\tau_{copy} \approx \tau_0$.
	Assumptions: Universal update time τ_0; reversible local updates.		
	Sources: main manuscript; preprints202512.2120.v1		
MASS-1	Threshold for matter audit depth D_{audit}	$D_{audit} \geq 7$ in 3+1D for stable matter excitations	Explicit microscopic counterexample at $D_{audit} < 7$ within same axioms.
	Assumptions: Gauge-coded QCA; code-subspace stability.		
	Sources: preprints202512.2120.v1; 202512.2391 note		
MASS-2	Particle mass scales	$m_{eff} \propto (D_{audit}/\tau_{copy})$; predicts clustering at integer multiples of m_0	Experimental/analysis pipelines do not show such clustering under controlled re-analyses.
	Assumptions: Mass as certification cost; reference band m_0 from golden relation.		
	Sources: preprints202512.2391.v2 (scale clustering)		
ASTRO-1	Relative arrival-time lags	$\delta t(E, z)$ redshift integral controlled by $H(z)$ and $L_{copy}(t)$	Null constraints from GRB/AGN time-lag analyses; redshift dependence does not match.
	Assumptions: Same transient sector as DE-5; propagation over cosmological distances.		
	Sources: preprints202601.0639.v1 (Sec. 7)		
MASS-3	Collider exclusion bounds	Scales cluster and shift as $m_* \propto (D_{min}\tau_{min})^{-1/2}$	Re-analyses varying D_{min} do not shift the scale according to inverse-square-root law.
	Assumptions: Plateau regime for audit latency; θ and τ_{min} fixed.		
	Sources: preprints202512.2391.v2 (Eq. 8)		

Preprints.org (www.preprints.org) | NOT PEER-REVIEWED | Posted: 13 January 2026 doi:10.20944/preprints202601.0917.v1

ID	Observable	Prediction	Falsification route
CONST-1	Combination $\chi_Y^{(2)} T_*^2$	$\chi_Y^{(2)} T_*^2 = 0.145 \pm 0.010$	Independent lattice/FRG computation yields incompatible value.
Assumptions: FRG matching used in calibration layer; T_* defined by matching.			
Sources: preprints202511.2241.v4			
CONST-2	κ_{eff} in Golden Relation	$\kappa_{eff} = 0.136 \pm 0.019$	Microscopic computation yields κ_{eff} outside the interval.
Assumptions: Same calibration layer as CONST-1.			
Sources: preprints202511.2241.v4			
CONST-3	C_Λ constant	$C_\Lambda = 1.6 \pm 0.2\ \mathrm{GeV}^{-1}$	Independent derivation of C_Λ yields value outside uncertainty.
Assumptions: Same calibration layer as CONST-1.			
Sources: preprints202511.2241.v4			
DE-6	Joint consistency	Single $L_{copy}(z)$ must fit expansion, growth, and transient timing	No joint fit exists for any admissible τ_{copy} satisfying locality.
Assumptions: Framework mapping from τ_{copy} to L_{copy} and Ω_Q.			
Sources: preprints202601.0639.v1			
ASTRO-2	Redshift integral kernel	Residual lags must follow kernel fixed by $H(z)$ and $L_{copy}(z)$	Residuals show no redshift scaling or incompatible kernel.
Assumptions: Population-level marginalization removes intrinsic lags.			
Sources: preprints202601.0639.v1; predictions_catalog			
GR-4	Recovery of GR correlators	Micro model yields Einstein dynamics as IR scaling phase	Simulation shows absence of GR-like phase or produces non-diffeo-invariant correlators.
Assumptions: Discrete information-field action as specified.			
Sources: QICT_Supplement_Microscopic_GR.pdf			

References

1. Umegaki, H. Conditional expectation in an operator algebra. IV. Entropy and information. *Kodai Mathematical Seminar Reports* **1962**, *14*, 59–85.
2. Nielsen, M.A.; Chuang, I.L. *Quantum Computation and Quantum Information*; Cambridge University Press, 2010.
3. Helstrom, C.W. Quantum detection and estimation theory. *J. Stat. Phys.* **1969**, *1*, 231–252.
4. Fuchs, C.A.; van de Graaf, J. Cryptographic distinguishability measures for quantum-mechanical states. *IEEE Trans. Inf. Theory* **1999**, *45*, 1216–1227.
5. Jacobson, T. Entanglement equilibrium and the Einstein equation. *Phys. Rev. Lett.* **2016**, *116*, 201101.
6. Sakharov, A.D. Vacuum quantum fluctuations in curved space and the theory of gravitation. *Sov. Phys. Dokl.* **1968**, *12*, 1040–1041.
7. 't Hooft, G. *The Cellular Automaton Interpretation of Quantum Mechanics*; Springer, 2016.